Available online at www.sciencedirect.com
SCIENCE DIRECT®
European Journal of Medicinal Chemistry 38 (2003) 811–824
EUROPEAN JOURNAL OF MEDICINAL CHEMISTRY
www.elsevier.com/locate/ejmech

Original article

New styryl sulfones as anticancer agents☆

Manohar Sharma Vedula [a,*], Aravind Babu Pulipaka [a], Chandrasekhar Venna [a], Vamsee Krishna Chintakunta [a], Sreenu Jinnapally [a], Venkata Adiseshu Kattuboina [a], Ravi Krishna Vallakati [a], Vishnu Basetti [a], Venkateswarlu Akella [a], Sriram Rajgopal [b], Ajaya Kumar Reka [b], Sravan Kumar Teepireddy [b], Prem Kumar Mamnoor [b], Ramanujam Rajagopalan [b], Gopalakrishnan Bulusu [c], Akash Khandelwal [c], Vijay V. Upreti [d], Srinivas Rao Mamidi [d]

[a] *Discovery Chemistry, Discovery Research, Dr. Reddy's Laboratories, Bollaram Road, Hyderabad 500 050, India*
[b] *Discovery Biology, Discovery Research, Dr. Reddy's Laboratories, Bollaram Road, Hyderabad 500 050, India*
[c] *Molecular Modeling & Drug Design, Discovery Research, Dr. Reddy's Laboratories, Bollaram Road, Hyderabad 500 050, India*
[d] *Drug Metabolism & Pharmacokinetics, Discovery Research, Dr. Reddy's Laboratories, Bollaram Road, Hyderabad 500 050, India*

Received 20 January 2003; received in revised form 11 July 2003; accepted 11 July 2003

Abstract

New styryl sulfone compounds have been synthesized and evaluated for their anti-proliferative activity. Among the compounds synthesized, one compound (**7k**) has shown 51% tumor growth inhibition in mice implanted with HT-29 human carcinoma at 400 mg kg^{-1} orally.

Keywords: Substituted benzimidazole styryl sulfones; MAP kinase inhibitors; Anti-cancer activity

1. Introduction

Extra cellular signals received at transmembrane receptors and relayed into the cells by the signal transduction pathways [1], have been implicated in a wide array of physiological processes such as induction of cell proliferation, differentiation or apoptosis [2]. The mitogen activated protein kinase (MAPK) cascade is a major signaling system by which cells transduce extra cellular cues into intracellular responses [3,4]. In mammalian cells, the extra cellular signal-regulated kinases (ERKs), ERK-1 and ERK-2 are the archetypal and best studied members of the MAPK family and are activated by phosphorylation on threonine/tyrosine residues by upstream dual specifying kinases [5–7]. The best understood MAPK pathway involves extra cellular signal regulated kinases, which constitute the Ras/Raf/MEK/ERK kinase cascade [8]. Once this pathway is activated by different stimuli, MAPK phosphorylates a variety of proteins including several transcription factors, which translocate into the nucleus and activate gene transcription. Negative regulation of this pathway could arrest the cascade of these events and will inhibit the proliferation of cancer cells.

Recently, it was reported [9] that certain styryl sulfone derivatives like FRI-20 inhibit the tumor cell growth and viability by inhibiting the MAPK signal transduction pathway. The compounds regulate the ERK and inhibit the proliferation of breast and prostate tumor cells in a dose-dependent manner without affecting normal cell growth. The cell growth inhibitory activity of this compound is dictated by the nature and position of the functional groups.

☆ DRL Publication No. 282.

* Correspondence and reprints.
E-mail address: sarmavm@drreddys.com (M.S. Vedula).

0223-5234/03/$ - see front matter
doi:10.1016/S0223-5234(03)00144-2

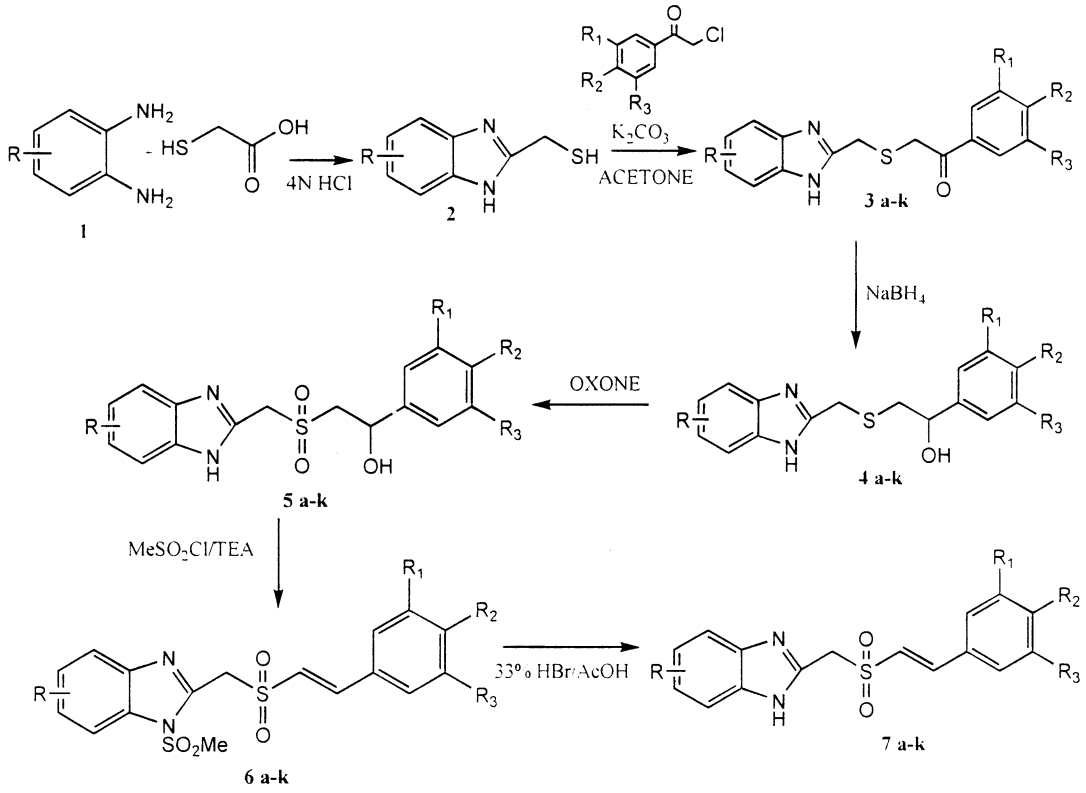

R=H, R_1,R_3=-$C(CH_3)_3$, R_2= -OH	**6a**	R=H, R_1,R_3=-$C(CH_3)_3$, R_2= -OH	**7a**
R=H, R_1=H, R_2=-OMe, R_3=H	**6b**	R=H, R_1=H, R_2=-OMe, R_3=H	**7b**
R=H, R_1=H, R_2=-Br, R_3=H	**6c**	R=H, R_1=H, R_2=-Br, R_3=H	**7c**
R=H, R_1=-CH_3, R_2=-F, R_3=H	**6d**	R=H, R_1=-CH_3, R_2=-F, R_3=H	**7d**
R=-6-Cl, R_1=-CH_3, R_2=-F, R_3=H	**6e**	R=-6-Cl, R_1=-CH_3, R_2=-F, R_3=H	**7e**
R=-6-Cl, R_1=-H, R_2=-Cl, R_3=H	**6f**	R=-6-Cl, R_1=-H, R_2=-Cl, R_3=H	**7f**
R=-H, R_1, R_2=-Cl, R_3=H	**6g**	R=-H, R_1, R_2=-Cl, R_3=H	**7g**
R=-H, R_1=-H, R_2=-Cl, R_3=H	**6h**	R=-H, R_1=-H, R_2=-Cl, R_3=H	**7h**
R=-H, R_1=-CH_3, R_2=-Cl, R_3=H	**6i**	R=-H, R_1=-CH_3, R_2=-Cl, R_3=H	**7i**
R=-6-Cl, R_1=-H, R_2=-F, R_3=H	**6j**	R=-6-Cl, R_1=-H, R_2=-F, R_3=H	**7j**
R=-6-Cl, R_1=-CH_3, R_2=-Cl, R_3=H	**6k**	R=-6-Cl, R_1=-CH_3, R_2=-Cl, R_3=H	**7k**

Fig. 1. Synthetic routes to compounds **7a**–**k**.

The objective of the present study is to synthesize novel styryl sulfone compounds exhibiting wide spectrum of activity and increased potency on different types of tumor cells both in-vitro and in-vivo. In order to facilitate the design and predict the activity of this new styryl sulfone compounds we performed a 3D QSAR study using comparative molecular similarity indices analysis (CoMSIA) [10,11]. We report here the synthesis, QSAR, in-vitro and in-vivo pharmacological evaluation and pharmacokinetic data of these compounds.

2. Chemistry

Synthesis of these compounds is outlined in Figs. 1 and 2. Commercially available *O*-phenylene diamines were condensed with thioglycolic acid to get 1H-benzo[d]imidazol-2-ylmethanethiol (**2**) which were further reacted with substituted phenacyl chlorides in presence of potassium carbonate in acetone to get 2-[{1H-benzo[d]imidazol-2-yl methyl}sulfanyl]-1-phenyl-1-ethanone (**3a**–**k**). These were easily converted to 2-[{1H-benzo[d]imidazol-2-ylmethyl}sulfanyl]-1-phenyl-1-

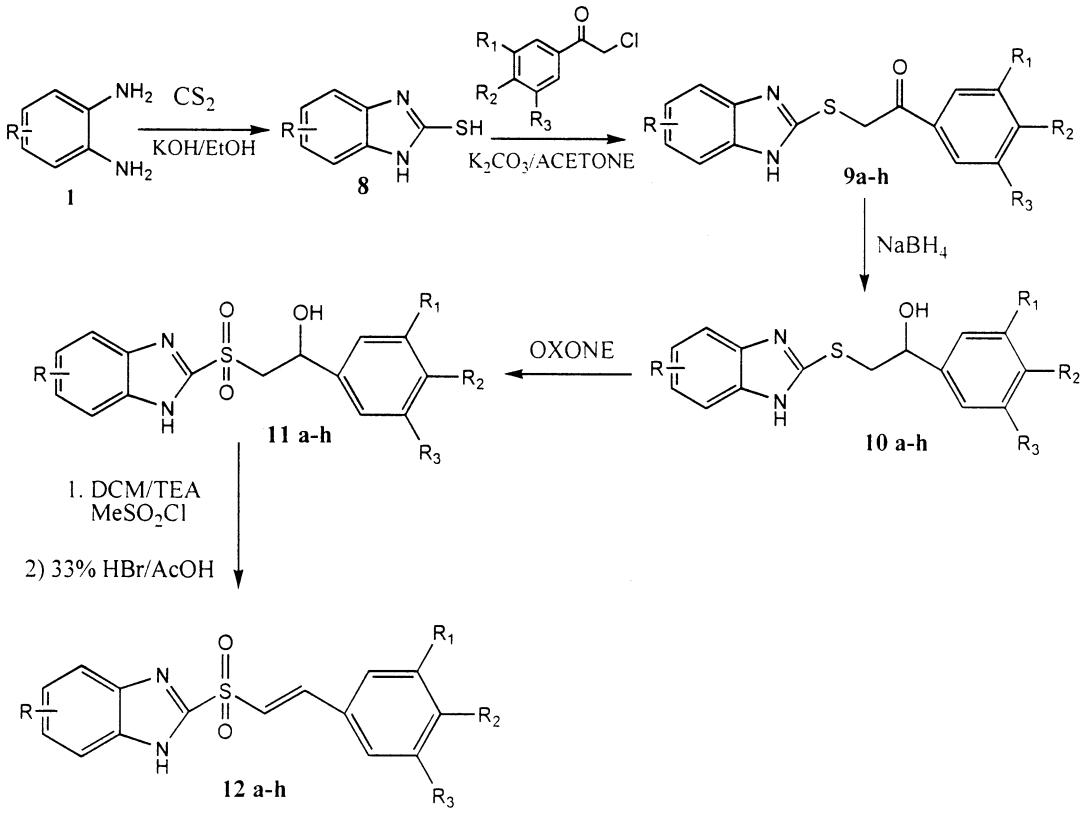

R=-H, R_1=-H, R_2=-Cl, R_3=-H	**12a**
R=-H, R_1=-CH_3, R_2=-F, R_3=-H	**12b**
R=-H, R_1=-CH_3, R_2=-Cl, R_3=-H	**12c**
R=-H, R_1=-H, R_2=-Br, R_3=-H	**12d**
R=-H, R_1=-H, R_2=-F, R_3=-H	**12e**
R=5-OCH_3, R_1=-H, R_2=-Br, R_3=-H	**12f**
R=5-OCH_3, R_1=-CH_3, R_2=-Cl, R_3=-H	**12g**
R=-H, R_1, R_3=-$C(CH_3)_3$, R_2=-OH	**12h**

Fig. 2. Synthetic routes to compounds **12a**–**h**.

ethanol (**4a**–**k**) by reduction with sodium borohydride. Compounds **4a**–**k** were oxidized to get 2-[{1H-benzo[d]imidazol-2-ylmethyl}sulfonyl]-1-phenyl-1-ethanol (**5a**–**k**). These compounds were subjected to dehydration with methane sulfonyl chloride to afford 1-{methylsulfonyl}-2-{([(*E*)-2-phenyl-1-ethenyl] sulfonyl}6a–**k**) which in turn were demesylated to 1H-benzo[d]imidazol-2-ylmethyl[(*E*)-2-phenyl-1-ethenyl]sulfones (**7a**–**k**) with 33% HBr in AcOH.

In a similar manner, 1H-benzo[d]imidazol-2-ylhydrosulfides (**8**) was prepared by condensing commercial *O*-phenylene diamine with carbon disulfide in the presence of potassium hydroxide and ethanol. Compound **8** was reacted with substituted phenacyl chlorides in potassium carbonate in acetone to get 2-{1H-benzo[d]imidazol-2-ylsulfanyl}-1-phenyl-1-ethanones (**9a**–**h**). These were reduced with sodium borohydride to afford 2-{1H-benzo[d]imidazol-2-ylsulfanyl}-1-phenyl-1-ethanol (**10a**–**h**), which subsequently were oxidized to 2-{1H-benzo[d]imidazol-2-ylsulfonyl}-1-phenyl-1-ethanol (**11a**–**h**). Dehydration with methane sulfonyl chloride followed by demesylation with 33% HBr in AcOH afforded 1H-benzo[d]imidazol-2-yl-[{*E*}-2-phenyl-1-ethenyl]sulfone (**12a**–**h**).

3. Results and discussion

All the compounds were evaluated for their in-vitro cytotoxic activity against different types of cancer cell lines. The tested compounds showed moderate to good cytotoxic activity and indeed, some of them were more potent than FRI-20. The compound **1** of this series showed weak anti-proliferative activity in the tested cell lines. Compounds substituted with halogens on the phenyl ring at the para position namely, **12d** and **12e**

Table 1
In-vitro anti-cancer activities (GI_{50} in μM) of compounds **12a**–**12h**

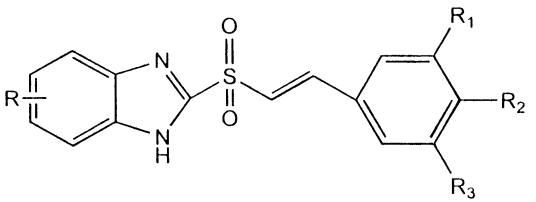

Compound	R	R_1	R_2	R_3	Breast		CNS	Colon		Lung	Melanoma	Ovarian		Prostate		Renal
					MCF7/ADR	MCF7	U251	SW620	HT29	H522	UACC62	SKOV3	PA1	DU145	PC3	A498
FRI-20					80	ND	9	6	ND	10	ND	50	ND	6	ND	9
12a	H	H	Cl	H	80	70	70	70	10	90	20	20	30	40	80	90
12b	H	CH_3	F	H	28	13	19	16	18	8	5	ND	15	20	ND	33
12c	H	CH_3	Cl	H	29	16	15	18	15	17	16	ND	15	28	ND	10
12d	H	H	Br	H	8	2	0.35	12	15	10	12	15	5	10	10	3
12e	H	H	F	H	18	4.5	8	1	20	0.06	2	ND	12	12	ND	100
12f	5OMe	H	Br	H	100	100	100	50	40	100	100	100	100	100	50	ND
12g	5-OMe	CH_3	Cl	H	100	100	ND	100	30	20	ND	35	100	25	20	12
12h	H	$C(CH_3)_3$	OH	$C(CH_3)_3$	0.35	0.3	ND	6.5	3.5	5	ND	15	2	10	7	5

ND, not done.

showed activity equal to the standard molecule FRI-20 (Table 1). It is interesting to note that **12d** with bromo substituent on the para position of the phenyl ring showed activity with an average GI_{50} of 8.5 μM. The compound showed significant activity particularly in breast (MCF-7), renal (A-498), CNS (U-251) and ovarian (PA1) cell lines. Compounds **12b** and **12c** were prepared to test the tolerability of further substitution *ortho* to the halo substituent. Unfortunately both the compounds failed to show appreciable cytotoxic activity. Further investigations were carried out to improve the activity of compounds in this series and it was found that 3,5-di-*tert*-butyl-4-hydroxy phenyl compound (**12h**) showed activity better than either unsubstituted or halo substituted benzimidazole derivatives. Compound **12h** showed a GI_{50} value of < 5 μM in most of the cell lines and also showed activity in adriamycin resistant breast cancer cell line indicating that these substituents play an important role in the cytotoxicity as predicted by QSAR studies. Compounds like **12f** and **12g** were also prepared with a methoxy group on the benzimidazole moiety. These compounds did not show any activity.

In continuation of SAR studies, compounds **7a** and **7h** (Table 2) were synthesized by incorporating an additional methylene between benzimidazole and sulfone moiety. Even though, **7h** showed better activity than **7a**, it was not comparable with **12h**. To check the tolerability of additional substitution on the imidazole ring, the free nitrogen in benzimidazole was substituted with a methyl sulfonyl group. All the compounds in this series **6a**–**j** failed to show activity (Table 3). Compound **7k** was found to be the most active in this series showing 50% growth inhibition in 4 cell lines at < 1 μM concentration. The pharmacokinetic properties in mice of **7k** and FRI-20 were studied and are summarized in Table 4. Compound **7k**, which has relatively good pharmaco kinetic properties, was selected for in-vivo experiments using human colon adenocarcinoma (HT-29) xenograft in nude mice. At 400 mg kg^{-1} dose compound **7k**, when administered orally, showed 51% tumor growth inhibition as shown in Fig. 3.

4. COMSIA studies

Partial least-square analysis (PLS) (Table 5) shows results obtained from atom based alignment. The atom-based alignment shows a cross-validated r^2 of 0.921 with five components, a non-cross-validated r^2 of 0.977, and standard error of estimate (s) of 0.057. The residual values of the training and test set molecules are shown in (Tables 6 and 7), respectively. The steric and electrostatic contour plots are shown in Fig. 4. The green regions indicate areas where steric bulk is predicted to enhance biological activity, whereas yellow contours indicate regions where steric bulk is predicted to be detrimental to biological activity. Blue colored regions indicate areas where electropositive groups are predicted to enhance biological activity, while red regions represent areas where electronegative groups are predicted to favor activity. The hydrophobic, hydrogen bond donor and hydrogen bond acceptor contours are displayed in Figs. 5 and 6, respectively. The hydrophobic fields (yellow, hydrophobic group favored; white, hydrophobic disfavored), H-bond donor (Cyan, favored; purple, disfavored) and the H-bond acceptor (magenta, favored; red, disfavored) fields indicate areas around the molecules where changes increased or decreased activity.

The higher activities of **12h** and **12a** as compared to other compounds may be due to the fact that the *t*-butyl substituent and the phenyl ring of **12h** and **12a** occupy green contours. The methyl group of compound **7k** occupies green contours and hence exhibits higher activity. The phenyl ring of **6j**, **6i**, **6g**, **6e**, **6d** and **6b** occupies yellow contours and hence exhibits lower activity. The cyan contour (H-bond favor) is embedded inside the purple contour (H-bond disfavored). The SO_2CH_3 group of **6j**, **6i**, **6g**, **6e** and **6b** touches cyan contour and protrudes out of purple contour. A graph of actual and predicted pGI_{50} values is shown in Fig. 7. The predictive power of each of the 3D-QSAR models was evaluated by predicting the pGI_{50} of 16 additional ligands not included in the training set. In all the cases, the predictive values fall close to the actual pGI_{50} values, deviating by not more than one logarithmic unit.

5. Conclusions

In conclusion, we have described the synthesis of a novel class of styryl sulfone compounds, their 3D QSAR studies using CoMSIA method and demonstrated that these compounds have potent anti-proliferative activity. Based on pharmacokinetic profiles we selected a compound **7k** for in-vivo studies. The in-vivo studies revealed that the compound showed efficacy against HT-29 human carcinoma inhibiting 51% tumor growth in a QDx20 schedule.

6. Experimental

6.1. Chemistry

The reported molecules were synthesized in the Discovery Research department of Dr. Reddy's Laboratories. All other chemicals and reagents used in the synthesis were of reagent grade. Melting points were determined on an Electro thermal melting point apparatus (Buchi 535) and were uncorrected. Pre-coated silica gel plates (20 × 20 cm, silica gel 60 F_{254}, Merck) were used for TLC. ^{1}H-NMR spectra were recorded on

Table 2
In-vitro anti-cancer activities (GI_{50} in μM) of compounds **7a**–**7k**

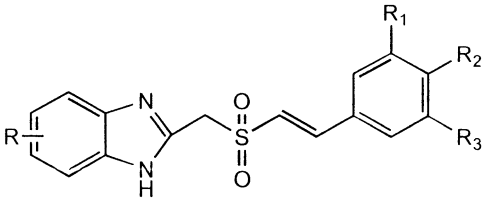

Compound	R	R_1	R_2	R_3	Breast		CNS	Colon		Lung	Melanoma	Ovarian		Prostate		Renal
					MCF7/ADR	MCF7	U251	SW620	HT29	H522	UACC62	SKOV3	PA1	DU145	PC3	A498
FRI-20					80	ND	9	6	ND	10	ND	50	ND	6	ND	9
7a	H	$C(CH_3)_3$	OH	$C(CH_3)_3$	20	100	100	100	100	100	100	ND	100	40	ND	15
7b	H	H	OMe	H	30	100	100	100	100	100	100	ND	10	30	ND	35
7c	H	H	Br	H	40	60	30	40	40	35	25	25	25	18	40	20
7d	H	CH_3	F	H	30	18	100	100	50	12	14	ND	19	52	ND	50
7e	6-Cl	CH_3	F	H	15	15	0.05	20	18	15	10	ND	15	3	ND	30
7f	6-Cl	H	Cl	H	25	0.02	15	18	18	15	15	ND	15	20	ND	20
7g	H	Cl	Cl	H	20	100	100	100	100	100	100	ND	100	2	ND	35
7h	H	H	Cl	H	45	45	20	25	30	30	20	30	30	20	25	20
7i	H	CH_3	Cl	H	15	50	30	30	35	20	20	20	20	30	25	30
7j	6-Cl	H	F	H	100	13	3	13	30	13	12	ND	100	100	ND	35
7k	6-Cl	CH_3	Cl	H	25	0.03	0.01	10	15	0.15	0.3	ND	16	13	ND	30

ND, not done.

Table 3
In-vitro anti-cancer activities (GI_{50} in μM) of compounds **6a**–**k**

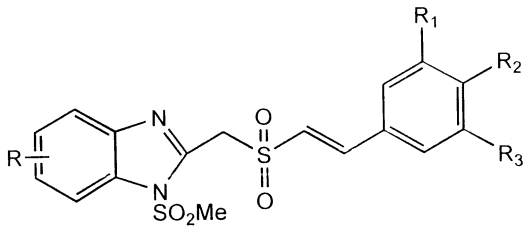

Compound	R	R_1	R_2	R_3	Breast		CNS	Colon		Lung	Melanoma	Ovarian		Prostate		Renal
					MCF7/ADR	MCF7	U251	SW620	HT29	H522	UACC62	SKOV3	PA1	DU145	PC3	A498
FRI-20					80	ND	9	6	ND	10	ND	50	ND	6	ND	9
6a	H	$C(CH_3)_3$	OH	$C(CH_3)_3$	4.5	60	4.5	5	5.5	30	18	100	3.5	4.5	30	60
6b	H	H	OMe	H	60	30	70	100	100	70	40	30	20	35	100	90
6c	H	H	Br	H	20	30	25	45	40	30	20	20	20	18	40	18
6d	H	CH_3	F	H	100	100	50	100	100	100	55	100	20	25	100	100
6e	6-Cl	CH_3	F	H	100	90	30	50	60	40	25	15	20	20	60	15
6f	6-Cl	H	Cl	H	35	65	20	25	25	25	20	18	20	20	20	20
6g	H	Cl	Cl	H	100	100	25	100	100	40	35	25	15	20	100	30
6h	H	H	Cl	H	30	40	25	80	45	25	25	30	20	20	60	30
6i	H	CH_3	Cl	H	100	100	100	100	100	100	100	4.5	30	30	100	70
6j	6-Cl	H	F	H	80	65	35	100	90	90	40	35	20	15	35	12
6k	6-Cl	CH_3	Cl	H	80	90	90	100	100	100	60	35	20	30	15	100

ND, not done.

Table 4
Pharmacokinetic parameters of **7k** and FRI-20 in mice at 100 mg kg^{-1}

	FRI-20	**7k**
$AUC_{(0-t)}$ (μg h mL^{-1})	1.27	10.57
$AUC_{(0-\infty)}$ (μg h mL^{-1})	1.95	11.80
C_{max} (μg mL^{-1})	0.35	9.90
T_{max} (h)	2.00	0.50
K_{el} (h^{-1})	0.21	0.27
$t_{1/2,\beta}$ (h)	3.34	2.57

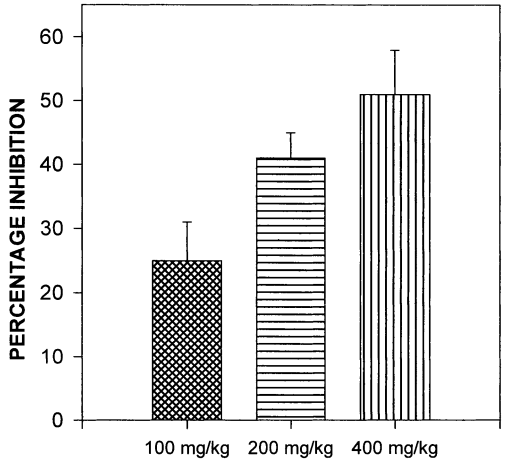

Fig. 3. Xenograft data of **7k**.

Table 5
Summary of PLS analysis

	CoMSIA
r^2_{cv}	0.921
r^2_{conv}	0.977
SEE	0.057
N	5
SDEP	0.106
Field contributions (%)	
Steric	13.7
Electrostatic	24.1
Hydrophobic	29.5
Donor	23.6
Acceptor	9.1

SEE, standard error of estimate; r^2_{cv}, cross-validated correlation coefficient; r^2_{conv}, non-cross-validated correlation coefficient; *N*, optimum number of components; SDEP, standard error of prediction.

Table 6
Actual and predicted pGI_{50} values of training set molecules

S. No.	Code	Actual pGI_{50}	Predicted pGI_{50}	Residuals
1	**6l**	4.6383	4.6401	−0.0018
2	**7i**	4.5686	4.5866	−0.0180
3	**7h**	4.5528	4.5366	0.0162
4	**6j**	4.2924	4.3472	−0.0548
5	**7c**	4.4815	4.6189	−0.1374
6	**6i**	4.1079	4.1405	−0.0326
7	**6g**	4.2366	4.1940	0.0426
8	**6e**	4.3565	4.3208	0.0357
9	**6d**	4.1024	4.1839	−0.0815
10	**6b**	4.2076	4.2229	−0.0153
11	**6m**	4.2007	4.1683	0.0324
12	**6n**	4.1871	4.1700	0.0171
13	**12c**	4.7696	4.6847	0.0849
14	**7f**	4.7959	4.7921	0.0038
15	**7e**	4.8239	4.8558	−0.0319
16	**12i**	4.7696	4.7583	0.0113
17	**12e**	4.7447	4.7092	0.0355
18	**12j**	4.6383	4.6049	0.0334
19	**12h**	5.3010	5.3074	−0.0064
20	**12a**	5.0458	5.0359	0.0099
21	**12f**	5.0398	5.0165	0.0233

Table 7
Actual and predicted pGI_{50} values of test set molecules

S. No.	Code	Actual pGI_{50}	Predicted pGI_{50}	Residuals
1	**7m**	4.0555	4.7447	−0.6892
2	**6o**	4.5229	4.2818	0.2411
3	**6h**	4.4437	4.1812	0.2625
4	**6f**	4.5850	4.3071	0.2779
5	**6c**	4.5686	4.1527	0.4159
6	**6a**	4.5686	4.1376	0.4310
7	**7g**	4.1549	4.6368	−0.4819
8	**7b**	4.1739	4.7386	−0.5647
9	**7a**	4.0969	4.6894	−0.5925
10	**7l**	4.5686	4.5884	−0.0198
11	**7d**	4.4089	4.7263	−0.3174
12	**7j**	4.3768	4.8347	−0.4579
13	**12b**	4.7696	5.0525	−0.2829
14	**7k**	5.0000	4.8105	0.1895
15	**12g**	4.2676	4.6621	−0.3945

a Varian-200 MHz, Gemini-200-software spectrometer (Varian USA). TMS was used as internal standard and chemical shifts are given in ppm. IR Spectra were recorded on a Perkin Elmer 1600 series FT IR (Perkin–Elmer, USA). Mass spectra were recorded on a Hewlett Packard 5989-A mass spectrometer. Starting materials were either commercially available or synthesized according to known literature methods.

*6.1.1. General procedure for the synthesis of 1H-benzo[d]imidazol-2-yl methanethiol (**2**)*

Commercially available *O*-phenylene diamines (**1**) (0.04 mol) and thioglycolic acid (0.04 mol) were added to 4 N HCl (120 mL) and contents were stirred at reflux temperature for 5 h. The mixture was basified with aq. sodium bi-carbonate solution till pH 10 and the solid precipitated was filtered to get 1H-benzo[d]imidazol-2-yl methanethiol as a solid.

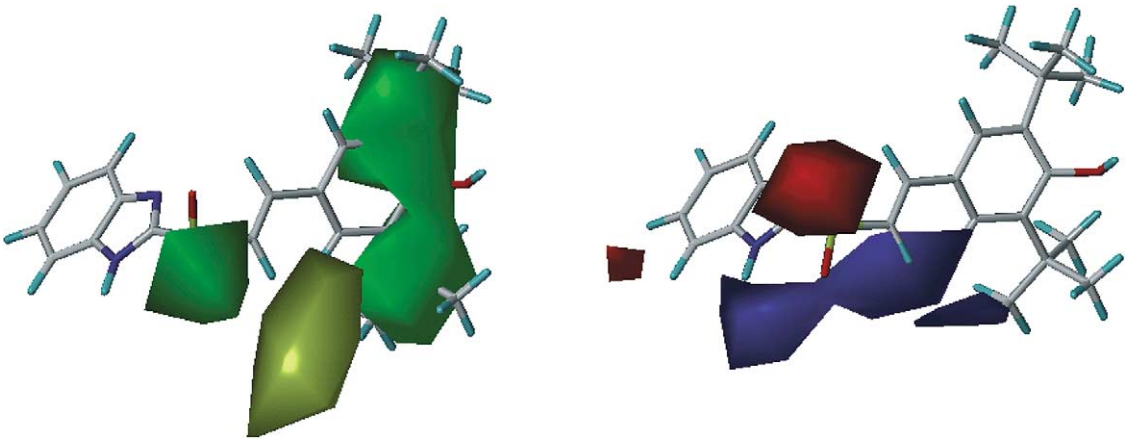

Fig. 4. CoMSIA stdev*coeff. Regions favoring bulkier substituents are represented by green contours while regions disfavors for bulky groups are represented by yellow contours. Areas favoring positive charges are represented by blue contours while negative charges are represented by red contours.

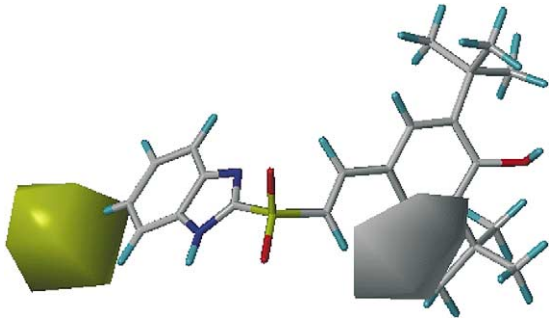

Fig. 5. CoMSIA stdev*coeff. Hydrophobic contour plots; yellow contours indicate regions where hydrophobic groups increases activity, whereas white contours indicate regions where hydrophobic group decreases activity.

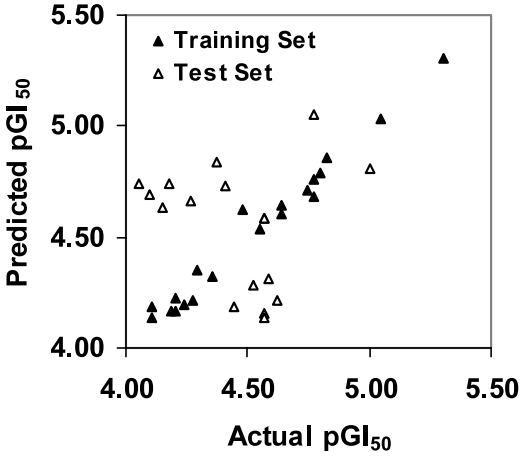

Fig. 7. Graph of actual vs. predicted pGI_{50} of training and test set molecules for CoMSIA 3D QSAR model.

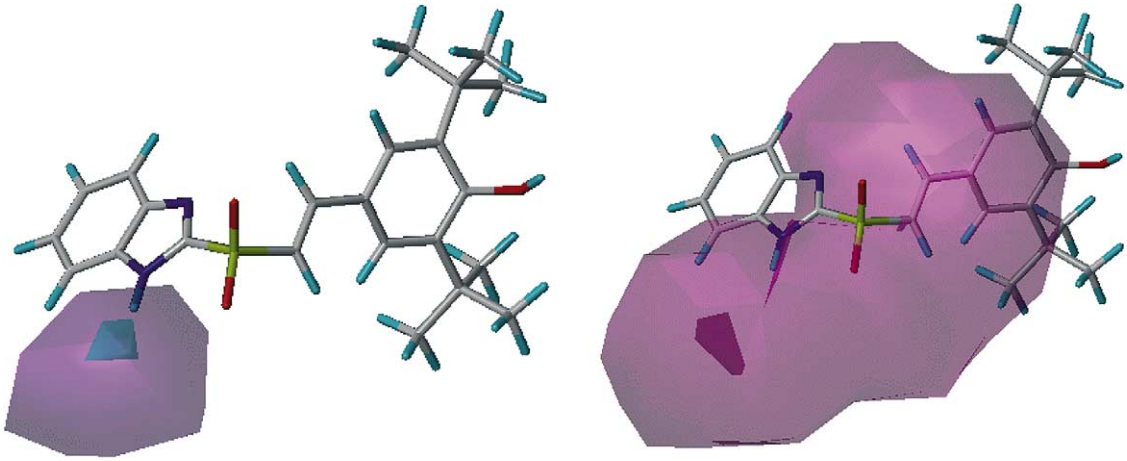

Fig. 6. CoMSIA stdev*coeff H-bond donor and acceptor plots: cyan contours indicate regions where H-bond donor group increases activity, whereas purple contours indicate regions where H-bond donor group decreases activity. Magenta contours indicate regions where H-bond acceptor group increases activity, whereas red contours indicate regions where H-bond acceptor group decreases activity.

*6.1.2. General procedure for the synthesis of 2-[{1H-benzo[d]imidazol-2-ylmethyl}sulfanyl]-1-phenyl-1-ethanone (**3a–j**)*

NaH (60%, 21 mmol) was added to a solution of 1H-benzo[d]imidazol-2-ylmethanethiol (**2**) (7 mmol) in 15 mL of DMF at 0 °C and the contents were stirred for 10 min. Appropriate phenacyl chloride (7 mmol) was added to the reaction mixture and contents were stirred for 2 h at room temperature (r.t.). Cold water (100 mL) was added to the reaction mixture and solid precipitated was filtered to give 2-[{1H-benzo[d]imidazol-2-ylmethyl}sulfanyl]-1-phenyl-1-ethanone.

*6.1.3. General procedure for the synthesis of 2-[{1H-benzo[d]imidazol-2-ylmethyl}sulfanyl]-1-phenyl-1-ethanol (**4a–j**)*

Sodium borohydride (8.1 mmol) was added slowly to a solution of 2-[{1H-benzo[d] imidazol-2-yl methyl}sulfanyl]-1-phenyl-1-ethanone (**3**) (2.7 mmol) in 20 mL of 1:1 chloroform and methanol at 0 °C and the contents were stirred for 30 min at r.t. Water (50 mL) was added to reaction mixture and extracted with ethyl acetate. The organic layer was evaporated to give 2-[{1H-benzo[d]imidazol-2-yl methyl}sulfanyl]-1-phenyl-1-ethanol.

*6.1.4. General procedure for the synthesis of 2-[{1H-benzo[d]imidazol-2-yl methyl}sulfonyl]-1-phenyl-1-ethanol (**5a–j**)*

Potassium mono persulphate triple salt (5.5 mmol) was added to a solution of 2-[{1H-benzo[d]imidazol-2-ylmethyl}sulfanyl]-1-phenyl-1-ethanol (**4**) (2.7 mmol) in 1:1:1 dichloromethane:*tert*-butanol:water (30 mL) and contents were stirred at r.t. for 7 h. Water (50 mL) was added to reaction mixture and extracted with ethyl acetate. Evaporation of the organic solvent gave crude product. This crude was washed with acetone to give pure 2-[{1H-benzo[d]imidazol-2-ylmethyl}sulfonyl]-1-phenyl-1-ethanol.

*6.1.5. General procedure for the synthesis of 1-{methylsulfonyl}-2-{([(E)-2-phenyl-1-ethenyl]sulfonyl}methyl}-1H-benzo[d] imidazole (**6a–j**)*

2-[{1H-Benzo[d]imidazol-2-ylmethyl}sulfonyl]-1-phenyl-1-ethanol (**5**) (2.7 mmol) was taken in dichloro methane (20 mL), triethyl amine (5.5 mmol) was added and the contents were stirred for 15 min. Methane sulfonyl chloride (5.5 mmol) was added slowly to the reaction mixture at 0 °C and stirred for 45 min. Water (100 mL) was added to the reaction mixture and extracted with dichloro methane. Evaporation of the organic layer and purification of the residue by column chromatography over 100–200 mesh silica gel gave 1-{methylsulfonyl}-2-{([(*E*)-2-phenyl-1-ethenyl]sulfonyl-methyl}-1H-benzo[d] imidazole.

*6.1.6. General procedure for the synthesis of 1H-benzo[d]imidazol-2-ylmethyl[(E)-2-phenyl-1-ethenyl]sulfone (**7a–j**)*

Three milliliters of 33% HBr in AcOH was added slowly to 1-{methylsulfonyl}-2-{([(*E*)-2-phenyl-1-ethenyl]sulfonyl}methyl}-1H-benzo[d] imidazole (**6**) (2.3 mmol) at 0 °C and the contents were stirred at r.t. for 15 min. Ice was added to reaction mixture and the solid formed was filtered to give crude product. This was purified by column chromatography to give 1H-benzo[d]imidazol-2-yl methyl[(*E*)-2-phenyl-1-ethenyl]sulfone.

*6.1.7. Synthesis of 2,6-di(tert-butyl)-4-[(E)-2-({[1-(methylsulfonyl)-1H-benzo[d]imidazol-2-yl]methyl}sulfonyl)-1-ethenyl] phenol (**6a**)*

Yield (42%); m.p. 197–199 °C; IR (KBr) cm^{-1}: 3554.5, 3006, 2961, 2916, 1616, 1594, 1537, 1453, 1420, 1373, 1323, 1293, 1259, 1226, 1178, 1147, 1100; ^{1}H-NMR (DMSO-d_6), δ_H 7.2 (m, 7H, aromatic), 6.9 (d, 1H, $J = 15.4$ Hz, Ar), 5.8 (s, 1H, –OH), 5.2 (s, 2H, $-CH_2$), 3.8 (s, 3H, SO_2CH_3), 1.4 (s, 18H, di-*tert*-butyl); Mass (*m*/*z*) (DIP): 505 (M^+), 427 (100%), 363, 233.

*6.1.8. Synthesis of 2-({[(E)-2-(4-methoxyphenyl)-1-ethenyl] sulfonyl} methyl)-1-(methylsulfonyl)-1H-benzo[d]imidazole (**6b**)*

Yield (45%); m.p. 169–171 °C; IR (KBr) cm^{-1}: 3024, 2929, 1602, 1511, 1451, 1366, 1290, 1254, 1172, 1122; ^{1}H-NMR ($CDCl_3$), δ_H 7.2 (m, 7H, Ar), 6.8 (m, 3H, Ar), 5.2 (s, 2H, $-CH_2$), 3.8 (s, 3H, SO_2Me), 3.6 (s, 3H, CH_3); Mass (*m*/*z*) (DIP): 407 (M^+), 329 (100%), 265, 211.

*6.1.9. Synthesis of 2-({[(E)-2-(4-bromophenyl)-1-ethenyl] sulfonyl}methyl)-1-(methyl sulfonyl)-1H-benzo[d]imidazole (**6c**)*

Yield (45%); m.p. 199–201 °C; IR (KBr) cm^{-1}: 3009, 2930, 1622, 1586, 1487, 1450, 1368, 1328, 1240, 1108, 1057; ^{1}H-NMR ($CDCl_3$), δ_H 7.2 (m, 9H, Ar), 7.0(d,1H, $J = 15.6$ Hz, styryl), 5.2 (s, 2H, $-CH_2$), 3.8 (s, 3H, SO_2CH_3); Mass (*m*/*z*) (DIP): 457 (M^+), 457, 379, 241, 211, 190 (100%).

*6.1.10. Synthesis of 2-({[(E)-2-(4-fluoro-3-methylphenyl)-1-ethenyl]sulfonyl}methyl)-1-(methylsulfonyl)-1H-benzo[d]imidazole (**6d**)*

Yield (43%); m.p. 179–181°C; IR (KBr) cm^{-1}: 3064, 3022, 2938, 1624, 1592, 1527, 1502, 1452, 1408, 1363, 1308, 1155, 1226; ^{1}H-NMR ($CDCl_3$), δ_H 6.9 (m, 9H, Ar), 5.2 (s, 2H, $-CH_2$), 3.5 (s, 3H, SO_2CH_3) 2.2 (s, 3H, CH_3); Mass *m*/*z* (DIP): 409 (M^+), 331 (100%), 190.

*6.1.11. Synthesis of 6-chloro-2-({[(E)-2-(4-fluoro-3-methyl phenyl)-1-ethenyl]sulfonyl}methyl)-1-(methyl sulfonyl)-1H-benzo[d]imidazole (**6e**)*

Yield (35%); m.p. 194–195 °C; IR (KBr) cm^{-1}: 3018, 2932, 1607, 1501, 1368, 1302, 1234, 1168, 1125, 1048; ^{1}H-NMR ($CDCl_3$): δ_H 7.0 (m, 8H, Ar), 5.2 (s, 2H, $-CH_2$), 3.8 (s, 3H, SO_2Me), 2.2 (s, 3H,$-CH_3$); Mass *m/z* (DIP): 443 (M^+), 365 (100%), 301, 245, 167.

*6.1.12. Synthesis of 6-chloro-2-({[(E)-2-(4-chlorophenyl)-1-ethenyl]sulfonyl}methyl)-1-(methylsulfonyl)-1H-benzo[d]imidazole (**6f**)*

Yield (39%); m.p. 230–232 °C; IR (KBr) cm^{-1}: 3020, 2950, 1619, 1527, 1492, 1454, 1367, 1303, 1259, 1168, 1129, 1097; ^{1}H-NMR ($CDCl_3$): δ_H 7.2 (m, 9H, Ar), 7.0 (d, 1H, styryl, $J = 15.6$ Hz), 5.2 (s,2H, $-CH_2$), 3.8 (s, 3H, $-SO_2Me$); Mass (*m/z*) (DIP): 406 (M^+, 100%), 367, 303.

*6.1.13. Synthesis of 2-({[(E)-2-(3,4-dichlorophenyl)-1-ethenyl]sulfonyl}methyl)-1-(methylsulfonyl)-1H-benzo[d]imidazole (**6g**)*

Yield (44%); m.p. 194–196 °C; IR (KBr) cm^{-1}: 3026, 2854, 1614, 1584, 1467, 1371, 1302, 1251, 1172, 1129; ^{1}H-NMR ($CDCl_3$), δ_H 7.0 (m, 9H, Ar), 5.2 (s, 2H, $-CH_2$), 3.8(s, 3H, $-SO_2CH_3$); Mass (*m/z*) (DIP): 445 (M^+), 367 (100%), 333, 303, 211.

*6.1.14. Synthesis of 2-({[(E)-2-(4-chlorophenyl)-1-ethenyl]sulfonyl}methyl)-1-(methylsulfonyl)-1H-benzo[d]imidazole (**6h**)*

Yield (45%); m.p. 189–191 °C; IR (KBr) cm^{-1}: 3022, 1591, 1490, 1449, 1365, 1295, 1170, 1126, 1053, 1013; ^{1}H-NMR ($CDCl_3$), δ_H 7.7(dd, 2H, $J = 9.2$ Hz, Ar), 7.3 (m,7H, Ar), 7.0 (d,1H, $J = 15.6$ Hz, styryl), 5.2 (s, 2H, $-CH_2$), 3.6 (s, 3H); Mass (*m/z*) (DIP): 411(M^+), 333, 269, 211, 133, 104, 94.

*6.1.15. Synthesis of 2-({[(E)-2-(4-chloro-3-methylphenyl)-1-ethenyl]sulfonyl}methyl)-1-(methylsulfonyl)-1H-benzo[d]imidazole (**6i**)*

Yield (45%); m.p. 204–206 °C; IR (KBr) cm^{-1}: 3423, 3058, 3022, 2939, 1620,1527, 1483, 1452, 1363, 1307, 1246, 1168; ^{1}H-NMR ($CDCl_3$), δ_H 7.7 (m, 2H, Ar), 7.2 (m, 6H), 7.0 (d, 1H, $J = 15.2$ Hz, styryl), 3.6 (s, 3H), 2.4 (s, 3H); Mass (*m/z*) (DIP): 425 (M^+), 347, 283, 211, 195, 185, 165, 153, 133 (100%), 112.

*6.1.16. Synthesis of 6-chloro-2-({[(E)-2-(4-fluorophenyl)-1-ethenyl]sulfonyl}methyl)-1-(methylsulfonyl)-1H-benzo[d]imidazole (**6j**)*

Yield (44%); m.p. 196–98 °C; IR (KBr) cm^{-1}: 3443, 3020, 2928, 1601, 1510, 1455, 1367, 1302, 1238, 1167, 1126; ^{1}H-NMR ($CDCl_3$) δ_H 7.1 (m, 8H, Ar), 7.0 (d, 1H, styryl, $J = 14.6$Hz), 5.2 (s, 2H, $-CH_2$), 3.6 (s, 3H, SO_2Me); Mass (*m/z*) (DIP): 429 (M^+), 391, 351 (100%), 287, 279, 254, 245, 231.

*6.1.17. Synthesis of4-{(E)-2-[(1H-benzo[d]imidazol-2-yl methyl} sulfonyl]-1-ethenyl}-2,6-di{tert-butyl} phenol (**7a**)*

Yield (50%); m.p. 142–144 °C; IR (KBr) cm^{-1}: 3610, 2963, 1713, 1674, 1616, 1548, 1439, 1362, 1310, 1225, 1201; ^{1}H-NMR ($CDCl_3$), δ_H 7.6 (m, 2H, Ar), 7–7.45 (m, 5H, Ar), 6.8 (d, 1H, $J = 15.6$ Hz, styryl), 6.2 (s, 1H, OH), 4.6 (s, 2H, CH_2), 1.4 (s, 18H, di-tert.butyl); Mass (*m/z*) (DIP): 427 (, M^+,100%), 362, 217, 132.

*6.1.18. Synthesis of 1-(1H-benzo[d]imidazol-2-yl methyl[(E)-2-{4-methoxy phenyl}-1-ethenyl]sulfone (**7b**)*

Yield (53%); m.p. 190–191 °C; IR (KBr) cm^{-1}: 3060, 3002, 2940, 2835, 1599, 1511, 1433, 1404, 1308, 1291, 1257, 1173; ^{1}H-NMR ($CDCl_3$), δ_H 7.2 (m, 7H, Ar), 6.6 (m, 3H, Ar), 4.8 (s, 2H, CH_2), 3.8 (s, 3H, OCH_3); Mass (*m/z*) (DIP): 329 (M^+, 100%), 264, 249, 149, 132.

*6.1.19. Synthesis of 1H-benzo[d]imidazol-2-yl methyl[{E}-2-(4-bromophenyl)-1-ethenyl]sulfone (**7c**)*

Yield (49%); m.p. 209–211 °C; IR (KBr) cm^{-1}: 3331, 3057, 1613.8, 1587, 1488, 1454, 1433, 1305;^{1}H-NMR ($CDCl_3$), δ_H 7.2 (m, 9H, Ar), 6.8 (d, 1H, styryl, $J = 15.2$ Hz), 4.8 (s, 2H); Mass (*m/z*) (DIP): 379 ($M^+ + 2$), 381 (M^+), 315, 299, 183, 133, 113.

*6.1.20. Synthesis of 1H-benzo[d]imidazol-2-yl methyl[{E}-2-(4-fluoro-3-methyl phenyl)-1-ethenyl]sulfone (**7d**)*

Yield (45%); m.p. 177–79 °C; IR (KBr) cm^{-1}: 3282, 3026, 2998, 1703, 1615, 1589, 1502, 1442, 1402, 1328, 1299, 1257, 1190, 1130; ^{1}H-NMR (DMSO-d_6+$CDCl_3$), δ_H 2.2 (s, 2H), 6.8 (d, 1H, $J = 8.4$ Hz), 7.0 (t, 1H, $J = 8$ Hz), 7.1–7.4 (m, 4H), 7.4–7.6 (m, 3H); Mass (*m/z*) (CI): 330 (M^+), 260, 132 (100%), 104, 91.

*6.1.21. Synthesis of 6-chloro-1H-benzo[d] imidazol-2-yl)methyl[(E)-2-(4-fluoro-3-methyl phenyl)-1-ethenyl]sulfone (**7e**)*

Yield (37%); m.p. 111–113 °C; IR (KBr) cm^{-1}: 3421, 2928, 1604, 1501, 1431, 1311, 1256, 1147, 1110; ^{1}H-NMR ($CDCl_3$): 2.2 (s, 3H), 4.8 (s, 2H), 6.7–7.8 (m, 8H); Mass (*m/z*) (CI): 365 (M^+), 300, 285, 165 (100%), 136, 109, 97.

*6.1.22. Synthesis of 6-chloro-1H-benzo[d]imidazol-2-yl)methyl[(E)-2-(4-chloro phenyl)-1-ethenyl sulfone (**7f**)*

Yield (33%); m.p. 187–185 °C; IR (KBr) cm^{-1}: 3384, 2928, 1616, 1591,1528, 1491, 1431, 1309, 1145; ^{1}H-NMR ($CDCl_3$): 4.8 (s, 2H), 6.8 (d,1H, $J = 16$ Hz), 7.2–7.8 (m,

8H); Mass (*m*/*z*) (CI): 366 (M^+), 302, 165 (100%), 140, 138, 102, 90.

*6.1.23. Synthesis of 1H-benzo[d] imidazol-2-yl methyl[(E)-2-(3,4-dichloro phenyl)-1-ethenyl] sulfone (**7g**)*

Yield (45%); m.p. 201–202 °C; IR (KBr) cm^{-1}:1607, 1584, 1528, 1469, 1437, 1366, 1292, 1200, 1128; ^{1}H-NMR ($CDCl_3$), δ_H 7.0 (m, 9H, Ar), 4.8 (s, 2H, $-CH_2$); Mass (*m*/*z*) (DIP): 366 (M^+, 10%), 302, 267, 131 (100%), 104.

*6.1.24. Synthesis of 1H-benzo[d]imidazol-2-yl methyl[(E)-2-(4-chloro phenyl)-1-ethenyl] sulfone (**7h**)*

Yield (50%); m.p. 208–210 °C; IR (KBr) cm^{-1}: 3056, 2999, 2360, 1615, 1491, 1453, 1433, 1408, 1306, 1245, 1140; ^{1}H-NMR ($CDCl_3$), δ_H 7.2 (m, 9H, Ar), 6.7 (d, 1H, styryl, $J = 15.4$ Hz), 4.7 (s, 2H, CH_2); Mass (*m*/*z*) (DIP): 333 (M^+), 268, 253, 131 (base peak).

*6.1.25. Synthesis of 1H-benzo[d]imidazol-2-yl methyl[(E)-2-(4-chloro-3-methyl phenyl)-1-ethenyl sulfone (**7i**)*

Yield (48%); m.p. 122 °C; IR (KBr) cm^{-1}: 3280, 3015, 3000, 1703, 1615, 1589, 1502, 1442, 1402, 1328, 1299, 1257, 1190, 1130; ^{1}H-NMR ($CDCl_3$), δ_H 7.0 (m, 8H), 6.8 (d, 1H, styryl, $J = 15.2$ Hz), 4.7 (s, 2H), 2.3 (s, 3H); Mass (*m*/*z*) (DIP): 347 (M^+, 100%), 327, 313, 283, 133.

*6.1.26. Synthesis of 6-chloro-1H-benzo[d]imidazol-2-yl)methyl[(E)-2-(4-fluoro phenyl)-1-ethenyl]sulfone (**7j**)*

Yield (37%); m.p. 116–118 °C; IR (KBr) cm^{-1}: 2927, 1599, 1510, 1449, 1328, 1233, 1158, 1040; ^{1}H-NMR ($CDCl_3$): 4.8 (s, 2H), 6.7–6.8 (d, 1H, $J = 15.8$ Hz), 7.2–7.8 (m, 8H); Mass (*m*/*z*) (CI): 350 (M^+), 286, 165 (100%), 138, 122, 101, 91.

*6.1.27. Synthesis of 6-chloro-1H-benzo[d]imidazol-2-yl)methyl[(E)-2-(4-chloro-3-methyl phenyl)-1-ethenyl]sulfone (**7k**)*

Yield (40%); m.p. 166–168 °C; IR(KBr) cm^{-1}: 3658, 3062, 2992, 2929, 2282, 1612, 1528, 1477, 1427; ^{1}HNMR (DMSO-d_6) 12.8 (s, 1H), 7.2–8.0 (m, 8H), 4.9 (s, 2H), 2.4 (s, 3H); Mass (*m*/*z*) (CI): 382 (M+2), 381 (M+1), 380 (M^+), 316, 167, 152.

*6.1.28. General procedure for the synthesis of 1H-benzo[d]imidazole-2-yl hydrosulfide (**8**)*

Potassium hydroxide (1 mmol), carbon disulfide (1 mmol) were added to commercially available *O*-phenylene diamine (1 mmol) in 10 mL of ethanol and the contents were refluxed for 3 h. Norit was added to the contents, refluxed for 15 min and filtered. Water (30 mL) was added to the filtrate and the solid precipitated was filtered to give 1H-benzo[d]imidazole-2-yl hydrosulfide.

*6.1.29. Synthesis of 1H-benzo[d]imidazol-2-yl[(E)-2-(4-chloro phenyl)-1-ethenyl sulfone (**12a**)*

Yield (35%); m.p. 235–37 °C; IR (KBr) cm^{-1}: 3387, 3247, 3040, 3000, 2920, 2850, 2581, 2293, 1918, 1747, 1605, 1563, 1487, 1405, 1355, 1332, 1226; ^{1}H-NMR (DMSO-d_6), δ_H 7.9 (t, 4H, $J = 8.2$ Hz, Ar), 7.7 (m, 2H), 7.5 (d, 2H, styryl, $J = 8.2$ Hz), 7.4 (m, 2H); Mass (*m*/*z*) (DIP): 319 (M^+, 100%), 254, 219, 159, 139, 119.

*6.1.30. Synthesis of 1H-benzo[d]imidazol-2-yl[(E)-2-(4-fluoro-3-methyl phenyl)-1-ethenyl sulfone (**12b**)*

Yield (30%); m.p. 208–209 °C; IR (KBr) cm^{-1}: 3282, 3026, 2998, 1703, 1615, 1589, 1502, 1442, 1402, 1328, 1299, 1257, 1190, 1130, 1003; ^{1}HNMR (DMSO-d_6+$CDCl_3$), δ_H 2.2 (s, 3H), 7–8 (m, 9H), 13.4 (brs, 1H); Mass (*m*/*z*) (DIP): 316 (M^+), 251, 133, 118 (100%), 115, 91.

*6.1.31. Synthesis of 1H-benzo[d]imidazol-2-yl-[(E)-2-(4-chloro-3-methyl phenyl)-1-ethenyl sulfone (**12c**)*

Yield (28%); m.p. 135–137 °C; IR (KBr) cm^{-1}: 2929, 1712, 1615, 1431, 1303, 1238, 1113; ^{1}H-NMR ($CDCl_3$), δ_H 2.4 (s, 3H), 4.9 (s, 2H), 6.9 (d, 1H), 7.2–7.7 (m, 8H); Mass (*m*/*z*) (DIP): 316 (M^+), 281, 166 (100%), 152, 115, 91.

*6.1.32. Synthesis of 1H benzo[d]imidazol-2-yl[(E)-2-(4-bromo phenyl)-1-ethenyl sulfone (**12d**)*

Yield (25%); m.p. 228–230 °C; IR (KBr) cm^{-1}: 3389, 3286, 1609, 1586, 1441, 1401, 1329, 1137, 1071; ^{1}H-NMR ($CDCl_3$+DMSO-d_6), δ_H 7–8 (m, 10H); Mass (*m*/*z*) (DIP): 364(M^+), 299, 218, 118(100%), 102, 90.

*6.1.33. Synthesis of 1H-benzo[d]imidazol-2-yl[(E)-2-(4-fluoro phenyl)-1-ethenyl sulfone (**12e**)*

Yield (30%); m.p. 217–218 °C; IR (KBr) cm^{-1}: 3265, 3007, 1616, 1599, 1510, 1443, 1329, 1233, 1194, 1162; ^{1}H-NMR (DMSO- d_6), δ_H 7–8 (m, 10H), 14 (brs, 1H); Mass (*m*/*z*) (DIP): 302 (M^+), 237, 118 (100%), 101, 90.

*6.1.34. Synthesis of (E)-2-(4-bromo phenyl)-1-ethenyl-(5-methoxy-1H-benzo[d]imidazol-2-yl)sulfone (**12f**)*

Yield (27%); m.p. 211–213 °C; IR (KBr) cm^{-1}: 3261, 3005, 2917, 2848, 1735, 1620, 1585, 1585, 1500, 1459, 1401, 1314; ^{1}HNMR (DMSO-d_6), δ_H 3.9 (s, 3H), 6.9–7.9 (m,9H); Mass (*m*/*z*)(DIP): 393 (M^+), 149, 99 (100%).

*6.1.35. Synthesis of (E)-2-(4-chloro-3-methyl phenyl)-1-ethenyl(5-methoxy-1H-benzo[d]imidazol-2-yl)sulfone (**12g**)*

Yield (25%); m.p. 205-207 °C; IR (KBr) cm^{-1}: 3256, 3000, 1611, 1510, 1477, 1327, 1200, 1160, 1133; ^{1}H-

NMR (DMSO-d_6), δ_H 2.2 (s, 3H), 3.9 (s, 3H), 6.9–8 (m, 8H); Mass (m/z) (DIP): 363 (M+2), 297, 191, 163, 149 (100%).

*6.1.36. Synthesis of 4-[(E)-2-(1H-benzo[d]imidazol-2yl sulfonyl)-1-ethenyl]-2,6-di(tert-butyl)phenol (**12h**)*

Yield (26%); m.p. 237–240 °C; IR (KBr) cm^{-1}: 3609, 3427, 3056, 2959, 1599, 1438 1422, 1332, 1273; ^{1}H-NMR ($CDCl_3$),δ_H 1.2 (s, 18H), 7–8 (m, 8H), 13.8 (s, 1H); Mass (m/z) (CI): 413 (M^+, 100%), 397, 357, 333, 311, 119.

6.2. Pharmacology

6.2.1. In vitro cell growth assay

Cells were seeded on a 96-well cell culture plates at a concentration of 10,000 cells/well in a volume of 100 μL of RPMI medium with 10% fetal bovine serum and were incubated at 37 °C in a CO_2 incubator. After 24 h cells were treated with varied concentrations of compound in 100 μL of medium and the control wells received vehicle. The plates were further incubated at 37 °C in a CO_2 incubator for 48 h. The assay was terminated by addition of 50% cold TCA to a final concentration of 10% to the cells, followed by incubation at 4 °C for 1 h. At the time of compound addition a separate set of cells having a 24 h growth were terminated for time zero growth (T_0). The TCA fixed plates were washed thrice with distilled water, air dried and stained with 0.4% SRB in 1% acetic acid for 30 min at room temperature. The plates were washed with 1% acetic acid, dried and the protein bound dye was dissolved in 100 μL of 10 mM Tris buffer and read at 515 nm. The percentage growth of treated cells is calculated compared to control with reference to time zero optical densities [12].

6.2.2. In vivo xenograft studies

CD-1 Nude mice were used for HT-29 (colon) human tumor xenografts. HT-29 tumors were initiated by implantation of tumor fragments (ca. 60 mm^3) from established tumors. Tumor fragments were implanted at s.c. into the axillary region of the animal. When the tumors reached a size of ca. 100 mm^3 experimental compounds were administered p.o. once daily for 20 days at 100, 200 and 400 mg kg^{-1} doses. The s.c. tumors were measured with calipers, and mice were weighed every alternate day and the volumes were calculated using the equation $V = (D \times d^2)/2$ where V (mg) is tumor volume, D is longest diameter in mm, and d is shortest diameter in mm [13]. Tumor volumes were converted into relative tumor volumes using the formula, Relative tumor volume = Average tumor volume on each reading day/Average tumor volume on starting day. From the relative tumor volumes the percentage tumor growth inhibition of compound treated animals compared to control was calculated using the formula,

$$\text{Percentage inhibition} = ((T_f - T_s)/(C_f - C_s)) \times 100$$

where T_f is the relative tumor volume of treated animals on final day, T_s is the relative tumor volume of treated animals on starting day, C_f is the relative tumor volume of control animals on final day and C_s is the relative tumor volume of control animals on starting day.

6.2.3. Determination of maximum tolerated dose (MTD)

To determine the MTD mice were grouped based on their body weights. The test compounds were formulated as suspension using appropriate vehicle and administered to the animals through oral route. The animals were observed for clinical signs of toxicity, body weight change for 14 days. Based on the mortality and body weight loss the MTD was calculated.

6.3. Pharmaco kinetic studies

Single dose oral pharmacokinetic studies for **7k** and FRI-20 were conducted in male Swiss albino mice (n = 12 animals for each compound, weight range: 20–26 g) at 100 mg kg^{-1} given in 0.25% CMC suspension. Blood samples were collected at predetermined time intervals over 0–24 h post-dose. Concentration of analyte was determined by suitable HPLC bioanalytical methods. Plasma concentration versus time profiles was generated over the 0–24 h time period and pharmacokinetic parameters were calculated based on non-compartmental analysis [14].

6.4. Molecular modeling

Molecular modeling and three-dimensional structure building were performed using SYBYL 6.8 [15] installed on a Silicon Graphics workstation with IRIX 6.5

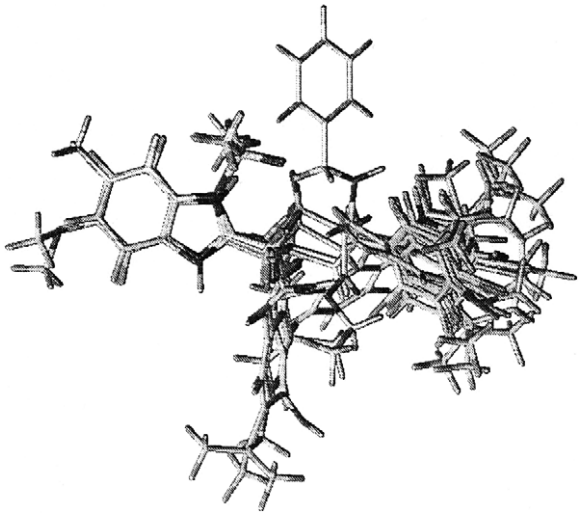

Fig. 8. Aligned molecules.

operating system. Energy minimizations were performed using Tripos force field with distance dependent dielectric and the Powell conjugate gradient method with a convergence criterion of 0.01 kcal mol^{-1}. Partial atomic charges were calculated using Gasteiger Huckel method. The CoMSIA method was employed for deriving 3D QSAR models for these compounds keeping activity pGI_{50} as a dependent variable. The conformations of the molecules used in the study were generated by systemic search method. Atom based alignment (RMS fit) was employed in this study. Compound **12h** was taken as a template and all the molecules were aligned on it using atoms of benzimidazole ring. The aligned molecules are shown in Fig. 8.

Acknowledgements

Spectral data recorded by the analytical group is gratefully acknowledged.

References

[1] S.L. Pelech, J.S. Sanghera, Science 257 (1992) 1355.
[2] R.J. Davis, J. Biol. Chem. 268 (1993) 14553.
[3] E. Nishida, Y. Gotoh, Trends Biochem. Sci. 18 (1993) 128.
[4] K.J. Blumer, G.L. Johnson, Trends Biochem. Sci. 19 (1994) 236.
[5] J. Posada, J.A. Cooper, Science 255 (1992) 212.
[6] W.H. Biggs, III, S.L. Zipursky, Proc. Natl. Acad. Sci. USA 89 (1992) 6295.
[7] A. Gartner, K. Nasmyth, G. Ammerer, Genes Dev. 7 (1992) 1280.
[8] B. Derijard, M. Hibi, I.H. Wu, T. Barrett, B. Su, T. Deng, M. Karin, R.J. Davis, Cell 76 (1994) 1025.
[9] V. Adler, C.C. Franklin, A.S. Kraft, Proc. Natl. Acad. Sci. USA 89 (1992) 5341.
[10] G. Klebe, U. Abraham, T. Mietzner, J. Med. Chem. 37 (1994) 4130.
[11] M. Bohm, J. Stuzerbercher, G. Kliebe, J. Med. Chem. 42 (1999) 458.
[12] A. Marks, D. Scudiero, P. Skehan, R. Shoemaker, K. Paull, D. Vistica, C. Hose, J. Langley, P. Cronise, A. Vaigro-Wolff, M. Gray-Goodrich, H. Campbell, J. Mayo, M. Boyd, J. Natl. Cancer Inst. 83 (1991) 757.
[13] D.W. Rusnak, K. Lackey, K. Affleck, Mol. Cancer Ther. 1 (2001) 85.
[14] M. Gibaldi, D. Perrier, J. Swarbrick, Pharmacokinetics, vol. 4, Marcel Dekker, New York, 1982, p. 149.
[15] SYBYL 6.8, Tripos Associates: St. Louis, MO, USA.